UNSYS digital

The Journal of Instrumentation, Automation and Systems

Pitch Oscillation Control of Hydroplane in Dual System of Lab-scale Flapping Type Tidal Energy Harvester

Indra H. Tambunan[†], Patar E. Sitorus[§], Hendra A. Putra[‡], Jin Hwan Ko[§], Hoon Cheol Park[‡], and Tae Sam Kang[†]

[†]Department of Aerospace Information Engineering, Konkuk University, Korea

[§]Department of Coastal & Environmental Engineering, Korea Institute of Ocean Science and Technology, Korea

[‡]Department of Advanced Technology Fusion, Konkuk University, Korea

Abstract—This paper describes the controller design of oscillation motion of hydroplane in dual-system lab-scale flapping type tidal energy harvester (FT-TEH).In dual-system, two identical single systems of lab-scale FT-TEH are arranged in a series with one chord length distance between the hydroplanes, wherein the flapping arm of each system is facing inwardly to each other. Both pitch noses direction of the hydroplanes are against the water flow. Controller is designed to control the motion of hydroplane such that each system moves in synchronized motion to each other at predetermined phase difference. Here, the system uses automatic gain controller with PID as the control feedback. Simulation and experiment results indicate that the controller of pitch oscillation for dual system of the lab-scale FT-TEH is well implemented.

Keywords—Tidal stream turbine, PID, flapping type turbine, control system.

I. Introduction

In recent time, there are several methods that have been developed to harness power from tidal energy. Horizontal axis turbine, as one of the most established tidal turbines, is based on the same principle of the widely used wind turbines. On the other hand, vertical axis turbines can cover a wider area in shallow water due to their geometry compared to the ones with horizontal axis. The vertical axis type turbine can be used more effectively when the stream speed is low because the cut-in speed of the vertical axis type turbine is lower compared with that of the horizontal axis type turbine. Several horizontal axis turbines [2,3] and vertical axis turbines [4,5] have been built and deployed. Despite all the advantages that the horizontal and the vertical axis turbines have, there are several disadvantages that could make these turbines uncompetitive. According to EPRI [6], horizontal and vertical axis turbines are economically viable in average flow velocity 5-7 knots or higher, while majority of sea currents around the world are less than 3 knots, and for river typically slower than 2 knots. Other disadvantages that these two methods have are high production and maintenance cost since all parts of the system are installed underwater.

Therefore, several researchers are working on other methods which could overcome the disadvantages of the well-developed aforementioned methods. Pulse-stream generator by Pulse Tidal Ltd. [7] and Stingray Tidal Stream Generator by IHC Engineering Business Ltd. [8] are some of examples of oscillating hydrofoil system in harnessing tidal stream energy. These systems can be implemented in shallow water because the length and width of the hydrofoil can be adjusted for a specific water stream given. Even though the hinge is installed underwater, the precision motion of the hinge is not required, and thus the implementation cost could be lowered. The Flapping Type Tidal Energy Harvester (FT-TEH), a kind of oscillating hydrofoil energy harvester, has the capability of increasing power extraction by just expanding the span of the hydroplane.

Research on extracting power using flapping hydrofoil has been investigated by several researchers previously. M.F. Platzer's group has been actively investigating how to extract power from flapping wing/oscillating hydroplane [9,10,11,12]. Liu *et al*. presented the flow visualization of an oscillating hydrofoil through fluid dynamics computation and experimental results to investigate hydrodynamic characteristic of an oscillating hydrofoil [13]. On the other hand, Abiru et al. reported that both power generation and efficiency were increased as the wing pitching oscillation was increased up to 50° [14]. However, there has been no record of work regarding the motion control of hydrofoil and maintaining the oscillation of hydrofoil with stability.

This paper demonstrates a controller design of oscillation motion of hydroplane in dual system of lab-scale FT-TEH. This work is preliminary research for a real system of FT-TEH. A modified automatic gain control scheme [15] with PID control is used to keep stable oscillation of the arm. Control system is built based on the characteristic single system of FT-TEH. Therefore, through Section 2 and 3, the single control system is to be explained first. Based on the single control system, dual control system is developed by combining two single systems.

Corresponding author: Tae Sam Kang (e-mail: tskang@konkuk.ac.kr).
This paper was submitted on September 29, 2014; revised on October 29, 2014; and accepted on December 18, 2014.

II. Dynamic Model of the FT-TEH

Dual system FT-TEH is the combination of two identical single system FT-TEHs. Therefore, dynamic model of the system is only presented for dynamic of a single system. The dynamic model is used to design the controller for a single system as well as for the dual system of lab-scale FT-TEH.

Dynamic model of the system is derived from schematic model which shown in **Figure 1**. Due to the relative flow velocity W, as the hydroplane pitch nose up, lift and drag force that acting on the hydroplane are given as follows:

$$L = \frac{1}{2}\rho C_L S[(V_\infty + l\dot{\psi}\sin\psi)^2 + l^2\dot{\psi}^2\cos^2\psi] \quad (1.a)$$

$$D = \frac{1}{2}\rho C_D S[(V_\infty + l\dot{\psi}\sin\psi)^2 + l^2\dot{\psi}^2\cos^2\psi] \quad (1.b)$$

where ψ, V_∞, ρ, C_L, C_D, and S are flapping arm angle, far-field water flow, water density, lift and drag coefficient, and hydroplane surface area, respectively.

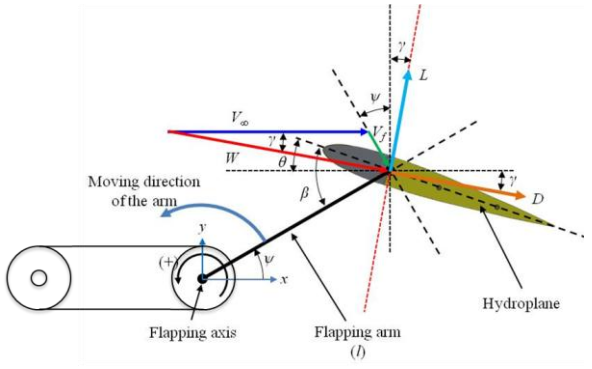

Figure 1 Schematic model of FT-TEH

Forces in x and y directions acting at the hydrodynamic center are defined as follow:

$$F_x = L\sin\gamma + D\cos\gamma \quad (2.a)$$

$$F_y = L\cos\gamma - D\sin\gamma \quad (2.b)$$

Moment due to the hydrodynamic force about the flapping axis is described as:

$$M = -F_x(l\sin\psi) + F_y(l\cos\psi) \quad (3)$$

Thus, by combining Equation 1, 2, and 3, the equation of motion of the system becomes:

$$(I + I_g)\ddot{\psi} + c\dot{\psi} - \frac{1}{2}\rho Sl[(V_\infty + l\dot{\psi}\sin\psi)^2 + l^2\dot{\psi}^2\cos^2\psi][(C_L\cos\gamma + C_D\sin\gamma)\cos\psi - (C_L\sin\gamma - C_D\cos\gamma)\sin\psi] = 0 \quad (4)$$

where, c is damping coefficient of the system. The I is mass moment of inertia of the hydroplane-flapping arm about the flapping axis, and the I_g is equivalent mass moment of inertia of the gear box about the axis of driving gear. The hydrodynamic analysis can be seen in the work of Truong *et al.* and Sitorus *et al.* [16, 17].

TABLE I
LAB-SCALE MODEL PARAMETER

Parameters	Value
ρ (kg/m^3)	997.13
I (kg.m^2)	0.0130
I_g(kg.m^2)	0.0019
S(m^2)	0.0435
c(kg.m^2/s)	0.45
V_∞(m/s)	0.6

Using lab-scale model parameters as shown in **TABLE I** and lift and drag coefficients of NACA0012 look up table from SANDIA [18], the transfer function of the system derived through *Matlab*® *Simulink* tools yields:

$$G(s) = \frac{\psi(s)}{\theta(s)} = \frac{594.9}{s^2 + 173.4s + 0.6274} \quad (5)$$

III. Controller Design and Simulation

The proposed scheme of automatic gain controller (AGC) in this work is shown in **Figure 2**. In this scheme, sum of output of feedback controller and nominal amplitude is multiplied by triangular wave function with the purpose of obtaining sinusoidal motion of ψ and θ. Nominal amplitude is used to invoke the oscillation of the flapping arm assuming no disturbances. The feedback control output is used to compensate for the disturbances including stream velocity change and non-modeled dynamics. This combination allows flapping motion of the arm moves continuously without being stalled. Direct feedback with proportional gain ε from the arm angle output ψ to the hydroplane pitch angle θ is introduced to keep the flapping motion of the arm centered at the zero angle position. A low pass filter is used to obtain smooth amplitude output, moving out the high frequency component, from the amplitude detector. The signal gain k_v is used to scale the signal in the loop.

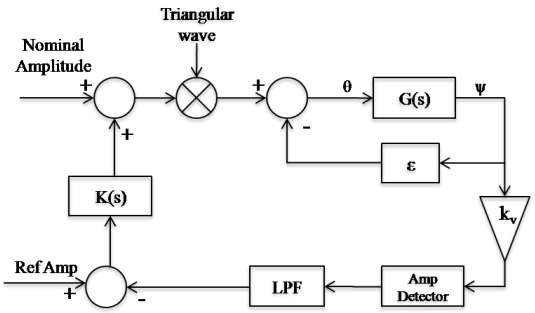

Figure 2 Configuration of modified automatic gain controller scheme

A. Dynamic Model Transformation

The AGC purpose is to regulate pitch amplitude of hydroplane motions with the given reference amplitude of flapping arm. Therefore, in order to control the amplitude of flapping arm, the system's transfer function modeled in Equation 5 needs to be remodeled into the amplitude terms.

Following the model plant in Equation 5, the plant's dynamic model can be expressed in the form:

$$\ddot{\psi} + a\dot{\psi} + b\psi = K_a\theta \tag{6}$$

Since the flapping arm's motion is the after effect of pitch hydroplane motion, a phase difference occurs between output angle of flapping arm motion and pitch hydroplane motion. Assuming that the driving frequency is near the resonance frequency of the system and considering the direct feedback from ψ to θ, the flapping arm motion and the pitching motion can be approximated as,

$$\begin{aligned} \psi(t) &= -B(t)\cos(\omega t) \\ \theta(t) &= -\varepsilon\psi(t) + A(t)\sin\omega t \end{aligned} \tag{7}$$

where, B(t) and A(t) are the time varying of amplitude of flapping arm and pitch-hydroplane respectively, ω is the frequency of the flapping arm motion. Then, by substituting the first and second derivative of $\psi(t)$ and $\theta(t)$ into Equation 6 and rearranging the sine term, the following gain equation is obtained:

$$2\omega\dot{B} + a\omega B = K_a A \tag{8}$$

Hence, by comparing Equation 5 and 8, the transfer function between the amplitude flapping arm and amplitude pitch-hydroplane is given as follows:

$$G_A(s) = \frac{B(s)}{A(s)} = \frac{594.9}{2.512s + 173.4} \tag{9}$$

Thus, the control block diagram of the system can be simplified as shown in **Figure 3**. Note that the gain of 2/π is introduced as a result of averaging the absolute value of sinusoidal signal envelope. The amplitude controller to be designed is denoted as *K(s)*.

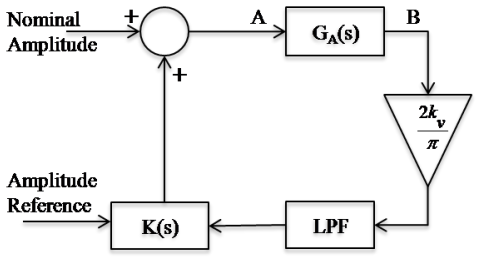

Figure 3 Simplified equivalent amplitude model of automatic gain control

B. PID controller

The form of PID controller in Laplace transform is given as follows:

$$K(s)L(S) = (K_p + \frac{K_i}{s} + K_d\frac{s}{s+1})(\frac{k_s}{\tau s+1}) \tag{10}$$

where the K_p, K_i, and K_d are proportional, integral and derivative gains, respectively. The τ and k_s are time constant and pass-band gain of first-order low-pass filter L(s), respectively. Based on the amplitude transfer function of the system as in Equation 9, the controller is designed by choosing the appropriate gains. The values of K_p, K_i, and K_d are chosen as 5, 0.05, and 0.1 respectively. The frequency responses are shown in **Figure 4**. The figure shows that the system has infinite gain margin and 121 degree phase margin. This is implies that the system is robustly stable with the designed controller. The bandwidth at approximately 3 rad/s is kept small since the amplitude response of the system is slow.

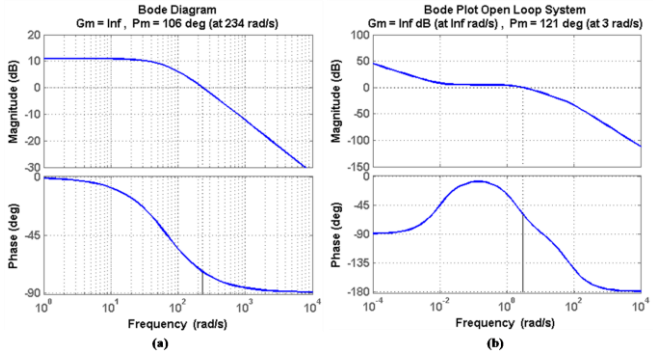

Figure 4 (a) Frequency responses of the plant and (b) Open loop plant with controller

C. Simulation

The simulation block of the control system with PID controller using *Matlab® Simulink* is built accordingly as shown in **Figure 5**. The controller used a nominal triangular wave signal to invoke a basic triangular motion of flapping arm angle ψ. A saturation block is used to keep pitch angle smaller than maximum limit. The maximum pitch angle is essential in the practical experiment to prevent system failure.

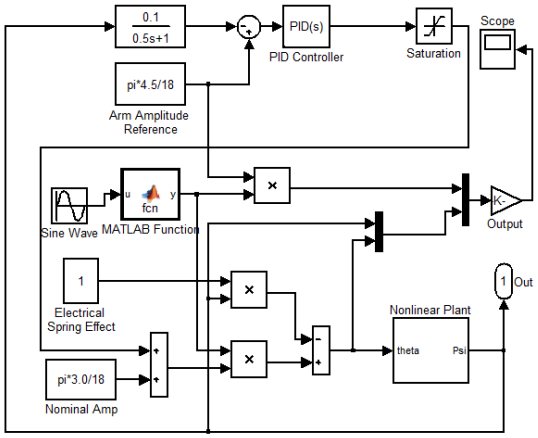

Figure 5 Schematic of simulation block with PID controller

The low pass filter L(s) = 0.1/(0.5s+1) is used to limit the bandwidth of the system. The arm amplitude reference is set to 45 degree for the reference motion of the flapping arm. The signal gain k_v is set to 1. The frequency of the triangular signal is set to 0.2 Hz as the system is to work in low frequency region.

The simulation result of the system with PID controller is shown in **Figure 6**. The result shows that the flapping arm follows the reference command quite well. The flapping arm oscillates symmetrically around zero flapping-arm angles as expected with the direct feedback spring effect with gain ε. As a result of the resonance characteristic between the two motions, 90 degree phase difference occurs between the flapping arm motion and the pitch hydroplane motion as expected.

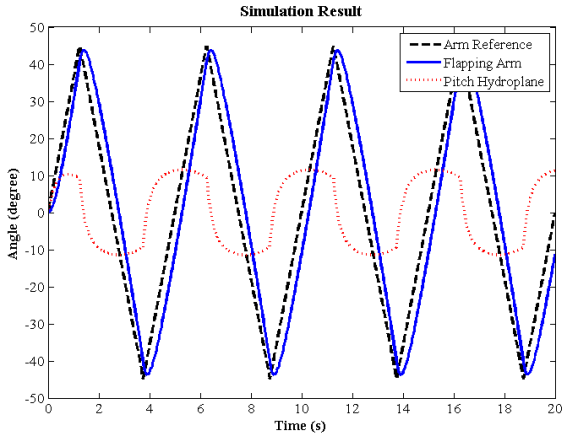

Figure 6 Simulation result using PID controller

IV. DUAL CONTROL SYSTEM AND IMPLEMENTATION

To extract more power from the sea current, we used dual FT-TEH system. Two FT-TEH systems are installed facing inward to each other, whereas the pitch noses of hydroplanes are facing the same direction against the water flow**.** The combination of this arrangement is shown in **Figure 7**.

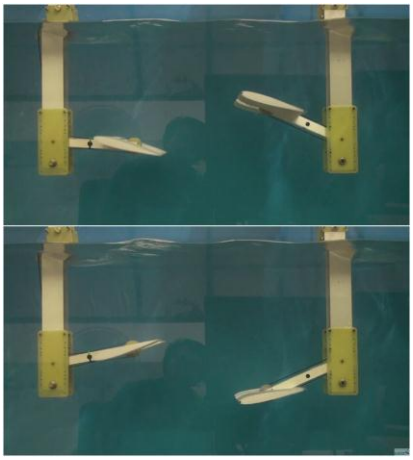

Figure 7 Snapshot of dual system configuration

Two microcontrollers (mbed® LPC1768) are used to control the two flapping systems. One is used as master and the other as slave. The slave hands over the arm angle and pitch angle information to the master. The master calculates control outputs for both flapping systems using arm angle information of both systems. And the slave drives the slave system using the control command from the master, while the master drives the pitch angle of the master system, as shown in Fig. 8. Two AC servo motors with the drivers (CN01 AC servo motors and FDA7001U drives from HIGEN motors) are used as the actuators. Two absolute rotary encoders from Autonics Inc. with series EPS50S8 are used to measure flapping arm angles of the two systems. **Figure 9** shows the brief diagram for the realization.

Serial communication RS-232 is used for the data exchange between the microcontroller and the servo driver, and CN1 connection is used for applying pulse and direction command to the servo motor system. Analog dials using potentiometers are used to give the input arm amplitude, nominal amplitude, frequency input, and offsets. The input dial can be easily changed by the users according to the condition of the experiments.

Based on the single control system, the dual control system is constructed as is shown in the flow chart in **Figure 8**. Dual system is divided into master control system to control the motion of hydro-plant 1 and slave control system to control hydro-plant 2. The main role of master control system is to obtain control outputs using all the information from both hydro-plant 1 and hydro-plant 2; and to give driving command to the slave control system through serial peripheral interface (SPI). Slave control system sends the information of hydro-plant 2 such as arm position and pitch position to master control system through SPI as well.

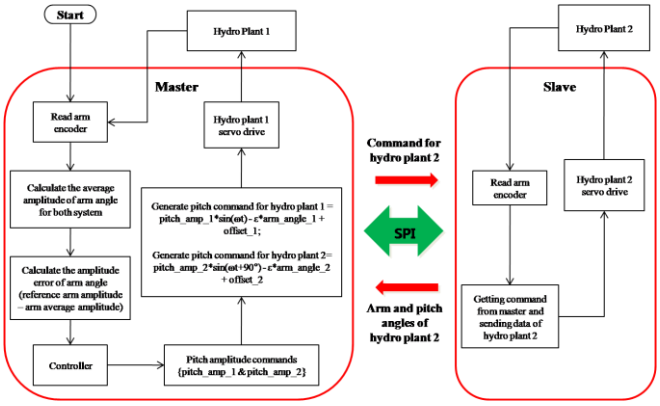

Figure 8 Flow chart for dual FT-TEH system

As the system starts, master control system gets the positions of arm angle of hydro-plant 1 and hydro-plant 2 using arm encoders. Then, master control system calculates the average amplitude of arm angle of each system. The controller gets the error amplitude of arm angle as an input and calculates the pitch amplitude. The pitch amplitude is modulated by the triangular wave to invoke triangular arm motions. The electrical spring effect of arm angle is added to the modulated signal to make the oscillation centered at zero arm position. The offset is given to compensate the bias due to asymmetries weight unbalance of the oscillating system. Then, the master control system generates the pitch command to the servo driver of hydro-plant 1 and sends the pitch command for hydro-plant 2 to the slave through SPI. The servo driver 1 and servo driver 2 drive the AC servo motors to make oscillating motion of the pitch of hydroplane of hydro-plant 1 and hydro-plant 2 separately.

All data information used for control is monitored through user interface utilizing LabVIEW™. The user interface displays the arm positions, pitch positions, frequency, offsets, and input command during experiments. Therefore, through this data, analysis of control system can be conducted.

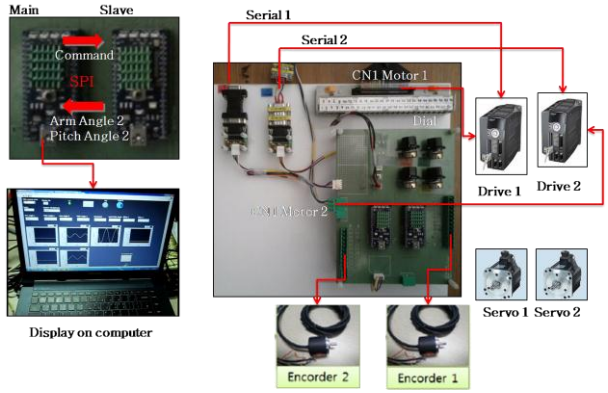

Figure 9 Implementation of control system for dual system FT-TEH

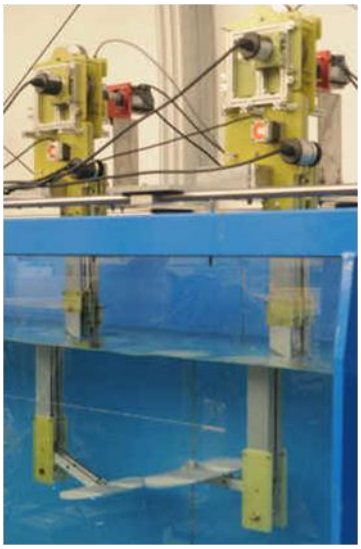

Figure 10 Dual system FT-TEH installations

V. Experiment and Result

A. Experiment Setup

Experiment was conducted in water channel at Korea Institute of Ocean Science and Technology. The cross section of water channel is 0.5m x 0.8m and the maximum average speed was 1m/s. A flow sensor (Quantum-X, HBN, Germany) was used to measure the water flow speed in the water tunnel, which was 0.6 m/s. A torque sensor (T20WN/1Nm, HBN, Germany) was installed at the output shaft of the gearbox. The holding torque applied to the output shaft was controlled by a torque control board and monitored using torque sensor DAQ. Dual FT-TEH system was installed such that the hydroplane is placed in the middle of the cross section. The installation of dual system is shown in **Figure 10**.

The given command for hydro-plant 1 and hydro-plant 2 has a phase difference of 90 degree wherein hydro-plant 2 is in the leading position. Amplitudes of the arm reference were set between 5 and 30, whereas nominal amplitudes are set between 10 and 15. The frequency input was set as 0.2 Hz.

B. Experiment Result

The experiment result of dual system FT-TEH is shown in **Figure 10**. The arm motion of hydro-plant 2 is leading that of hydro-plant 1 by 90 degrees.

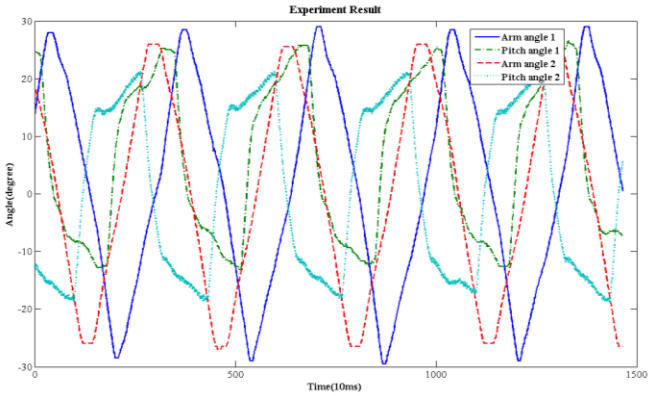

Figure 11 Experiment result of dual FT-THE system.

Figure 11 shows the experimental results. The flapping motions of the hydroplanes induced oscillating motions of the flapping arms. The pitch hydroplane 1 is not symmetrical at zero flapping angles due to the added offset. This added offset sets the arm flapping centered at the zero arm position. By setting the arm amplitude to 25, the amplitude of the flapping arm is desired to be 25 degrees. Experimental result shows that both of the arm amplitudes are kept around 25 degrees. Amplitude control experiment results for several different cases are shown in **Table II**.

TABLE II
AMPLITUDE ARM COMPARISON RESULT

Amp Arm Ref	Hydro-plant 1		Hydro-plant 2	
	B_1	A_1	B_2	A_2
5	8.5	10.5	5	10.5
	−7.5	−10.7	−5	−10.9
10	8.5	18.4	9.5	11.6
	−11.5	−4.4	−10.5	−10.7
15	16.5	23.8	15.5	15.4
	−18	−7	−14.5	−14
20	21.5	27.8	21	18.2
	−25.5	−7	−20.5	−17
25	24	25.7	26.5	20.1
	−33.3	−16.8	25	−19.4
30	38.5	28.7	30	27.3
	−37.5	−16.8	−32.5	−23.8

TABLE II shows the amplitude control results of hydro-plant 1 and hydro-plant 2. The A_i and B_i *(i=1, 2)* denote the pitch amplitude, and arm angle amplitude, respectively, of the hydro-plant *i*. It shows that the hydro-plant 2 follows the arm amplitude command better than hydro-plant 1. In the case of the hydro-plant 1, the down-stroke amplitudes of arm flapping are bigger than those of upstroke. This is due to the unbalance between the buoyancy forces and the weight of the flapping system.

Both pitch hydroplane and flapping arm motions show similarity to the simulation results that has been conducted, which demonstrates the validity of the simulation model.

VI. CONCLUDING REMARKS

Control system for dual system of lab-scale FT-TEH has been designed and implemented successfully. The simulation and experimental results demonstrated that the controller using automatic gain control with PID feedback could be used effectively to control the flapping motion of the arm.

ACKNOWLEDGMENT

This work was supported by the New & Renewable Energy R&D program of the Korea Institute of Energy Technology Evaluation and Planning (KETEP) under a grant funded by the Korea government Ministry of Trade, Industry and Energy (No. 20113020070010).

REFERENCES

[1] F. O. Rourke, F. Boyle, and A. Reynolds, " Tidal Energy Update 2009," *Applied Energy*, 2010, Vol. 87, pp. 398-409. CrossRef

[2] Industry Vision Paper 2013, European Ocean Energy, 2013. VIEW ITEM

[3] B. Kirkeand L. Lazauskas, "Variable Pitch Darrieus Water Turbines," Journal of Fluid Science and Technology, 2008, Vol.3, No.3.

[4] A. Schonborn and M. Chantzidakis, "Development of a hydraulic control mechanism for cyclic pitch marine current turbines", Renewable Energy, 2006, Vol. 32 pp.662-679. CrossRef

[5] S. H. Salter and J. R. M. Taylor, "Vertical-axis Tidal-Current Generators and the Penthland Firth," Proc. IMechE, Part A: J. Power and Energy, 2007, Vol.221.

[6] R. Bedard, M. Previsic, O. Siddiqui, G. Hagerman, M. Robinson, "Tidal in stream energy conversion (TISEC) devices," 2005, EPRI-TP-004NA.

[7] Pulse Generation Ltd. Hydrofoils or Turbines, 2008. VIEW ITEM

[8] Engineering Business Ltd., "Stingray Tidal Stream Energy Device – Phase 3," DTI and Future Energy Solutions, Contract Report ETSU T/06/00218/00/REP, UK, 2005.

[9] K. D. Jones, K. Lindsey, and M. F. Platzer, "An Investigation of the Fluid-Structure Interaction in an Oscillating-Wing Micro-Hydropower Generator," Fluid-Structure Interaction-II, WessexIn Technology Press, 2003, pp. 73-82.

[10] M. F. Platzer, J. Young, and J. C. S. Lai, "Flapping-wing Technology: The Potential for Air Vehicle Propulsion and Airborne Power Generation," *26th Congress of the International Council of the Aeronautical Sciences (ICAS)*, Anchorage, Alaska,14-19 Sep 2008.

[11] M. F. Platzer, M. A. Ashraf, J. Young, and J. C. S. Lai, "Extracting Power in Jet Stream: Pushing the Performance of Flapping Wing Technology,"*27th Congress of International Council of the Aeronautical Sciences*, Nice, France, 19 - 24 September 2010.

[12] M. A. Ashraf, J. Young, J.C.S. Lai, and M. F. Platzer, "Numerical Analysis of an Oscillating-Wing Wind and Hydropower Generator," AIAA Journal, 2011, Vol. 49, No. 7. CrossRef

[13] L. Zhen, H. Beom-soo, K. Moo-rong, and J. Ji-yuan, "Experimental and Numerical Study for Hydrodynamic Characteristic of an Oscillation Hydrofoil," Journal of Hydrodynamics, 2008, Vol. 20, No.3, pp. 280-287. CrossRef

[14] H. Abiruand A. Yoshitake, "Study on Flapping Wing Hydroelectric Power Generation System," Journal of Environment and Engineering, 2011, Vol. 6, No. 1, pp. 178-186. CrossRef

[15] W. T. Sung, S. K. Sung, J. G. Lee, T. S. Kang, "Design and performance test of a MEMS vibratory gyroscope with a novel AGC force rebalance control," Journal of Micromechanics and Microengineering, 2007, Vol. 17, pp. 1939-1948. CrossRef

[16] Q. T. Truong, P. E. Sitorus, I. H. Tambunan, H. A. Putra, H. C. Park, J. H. Ko, T. S. Kang, "Nonlinear dynamic model for flapping-type tidal energy harvester," Journal of Marine Science and Technology, ISSN No. 0948-4280, 2014. CrossRef

[17] P.E. Sitorus, T.Q. Le, J. H. Ko, Q. T. Truong, I. H. Tambunan, H. A. Putra, T. S. Kang, H. C. Park," Progress on development of a lab-scale flapping-type tidal energy harvesting system in KIOST(Published Conference Proceedings style)," IEEE Conference on Clean Energy and Technology (CEAT), Malaysia, 2013, pp. 42-47. CrossRef